Electron-Fluid Perturbation and Its Interaction with Electrons in a Field-Reversed Configuration*)

Fusaki P. IIZIMA, Toshiki TAKAHASHI, Takayuki WATANABE and Tomohiko ASAI[1)]

Department of Electronic Engineering, Gunma University, Gunma 376-8515, Japan

[1)]*College of Science and Technology, Nihon University, Tokyo 101-8308, Japan*

(Received 9 December 2011 / Accepted 5 April 2012)

Electron-fluid perturbation fields of a field-reversed configuration plasma is investigated by assuming the source of a electromagnetic wave is the electron current fluctuation. Electron trajectories in the prescribed perturbation field are calculated, and the toroidal flow velocity and velocity distribution and estimated by the particle-in-cell method. It is found that electrons are heated and enhancement of the end-loss of electrons is observed when the perturbation field is present.

Keywords: field-reversed configuration, electron-fluid perturbation, wave-particle interaction

DOI: 10.1585/pfr.7.2403057

1. Inroduction

The origin of resistivity in field-reversed configuration (FRC) plasmas has been unidentified as yet because of difficulties in diagnostic technique to measure pulsing events. In the history of transport study of FRC, the lower hybrid drift instability has believed to be the dominant process [1], however, it is disproved by Carlson's experiment [2]. Since obtainable data are restricted by an experimental approach, a numerical study is very convenient to investigate the transport phenomena in FRC plasmas. We are also interested in spontaneous toroidal spin-up mechanism, which may relate with resistive flux decay [3]. According to Ref. [3], the poloidal flux decrement directly changes to the kinetic angular momentum of both ions and electrons. If the current of both species increases, the poloidal flux maintains and no flux decay is observed. We suppose that the angular momentum of electrons is rapidly lost by some kind of transport mechanism. In the present paper, we assume the presence of electron fluid fluctuation with relatively high frequency, and study its interaction with electrons. Electron trajectories in the prescribed fluctuating fields are calculated, and response to the fluctuation and associated transport is discussed by collection of their motion.

2. Perturbation of Electron Fluid in an FRC

The wave equations of electromagnetic fields are

$$\nabla^2\phi - \frac{1}{c^2}\frac{\partial^2\phi}{\partial t^2} = -\frac{\rho}{\varepsilon_0}, \tag{1}$$

$$\nabla^2\boldsymbol{A} - \frac{1}{c^2}\frac{\partial^2\boldsymbol{A}}{\partial t^2} = -\frac{\boldsymbol{j}}{\varepsilon_0 c^2}. \tag{2}$$

author's e-mail: t-tak@el.gunma-u.ac.jp

*) This article is based on the presentation at the 21st International Toki Conference (ITC21).

Here, all the quantities above are fluctuating components and have the relations with the oscillating fields in the form

$$\boldsymbol{E}_1 = -\nabla\phi - \frac{\partial\boldsymbol{A}}{\partial t}, \tag{3}$$

$$\boldsymbol{B}_1 = \nabla\times\boldsymbol{A}. \tag{4}$$

Now, let us assume that the field perturbation is caused by plasma current fluctuations. Since an FRC plasma has a high beta value, the confinement field is sustained mainly by the plasma current containing fluctuation coming from typical electron motions. Since electrons are affected and ions are unable to follow, we choose the fluctuation frequency is $0.1\,\omega_{\mathrm{ec}}$, where ω_{ec} is the electron cyclotron frequency. Then the source terms in Eqs. (1) and (2) are given as

$$\rho = \tilde{\rho}(r,z)\exp\{\mathrm{i}(n\theta-\omega t)\}, \tag{5}$$

$$\boldsymbol{j} = \tilde{\boldsymbol{j}}(r,z)\exp\{\mathrm{i}(n\theta-\omega t)\}. \tag{6}$$

Amplitudes of $\tilde{\rho}(r,z)$ and $\tilde{\boldsymbol{j}}(r,z)$ are assumed to be proportional to the equilibrium quantities, then

$$\tilde{\rho}(r,z) = -\delta_n e n_{\mathrm{e}0}(r,z), \tag{7}$$

$$\tilde{\boldsymbol{j}}(r,z) = \delta_j \boldsymbol{j}_0(r,z). \tag{8}$$

The fluctuation ratios δ_n and δ_j are chosen small values, such as 10^{-3}. There is no experimental evidence that fluctuating fields in an FRC plasma originate from the above assumptions (7) and (8). However, it is reasonable to consider that the current fluctuation amplitude would peak where the current itself is the maximum value. The potentials are also in the form as

$$\phi = \tilde{\phi}(r,z)\exp\{\mathrm{i}(n\theta-\omega t)\}, \tag{9}$$

$$\boldsymbol{A} = \tilde{\boldsymbol{A}}(r,z)\exp\{\mathrm{i}(n\theta-\omega t)\}. \tag{10}$$

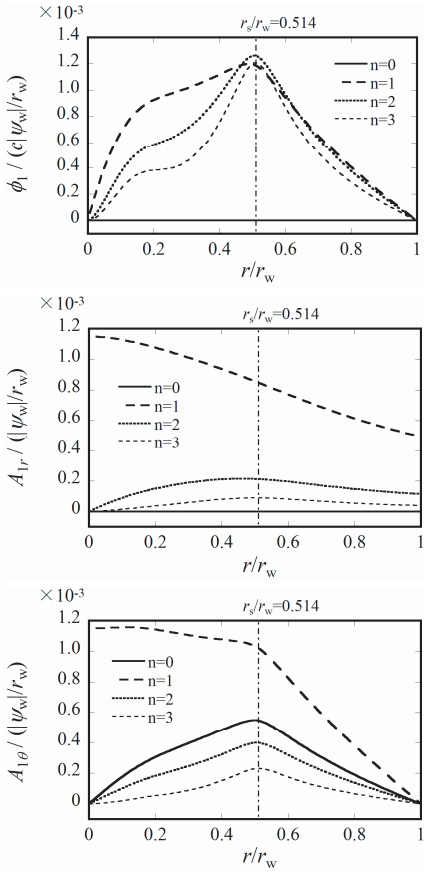

Fig. 1 The spatial profiles of the amplitude of the scalar and vector potentials on the midplane. (Top) the scalar potential, (middle) the radial component of vector potential, (bottom) the azimuthal component of vector potential. The separatrix position is indicated by the vertical dashed-dotted line.

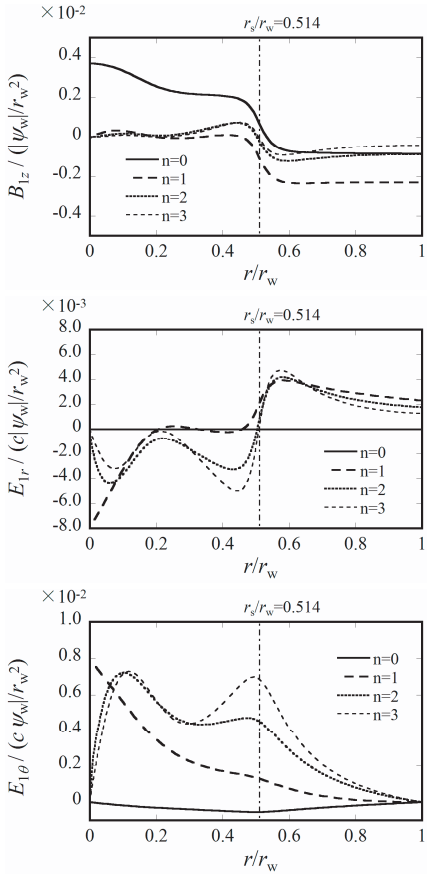

Fig. 2 The spatial profiles of the amplitude of electromagnetic wave caused by electron fluid perturbation. (Top) axial magnetic field, (middle) radial electric field, (bottom) azimuthal electric field.

The wave equations of potential are expressed by the cylindrical coordinates system. Assumption (8) gives $j_r = j_z = 0$ because an FRC plasma is sustained by only the toroidal current. We solve the equations for the amplitudes of fluctuating quantities by the finite difference method. Here, an equilibrium current profile is needed, and we obtained it by solving the Grad-Shafranov equation. The form of pressure function and the boundary conditions are the same as Ref. [4], and plasma parameters, such as, the plasma size, the confinement field, the temperature, etc. are determined by reference to the FRC experiment on the NUCTE-III [5].

The obtained spatial profiles of the scalar (ϕ_1) and vector potentials (A_{1r} and $A_{1\theta}$) on the midplane are shown in Fig. 1, where the profiles are drawn for the toroidal mode number n of 0, 1, 2, 3, and 4. In Fig. 1, ϕ_1 is normalized by $c|\psi_w|/r_w$, where c is the velocity of light, r_w is the chamber wall radius, and ψ_w is the flux function on the wall. The vector potentials are also normalized by $|\psi_w|/r_w$. For readers' convenience, the separatrix position is indicated by the vertical dashed-dotted line. No electrostatic potential arises for $n = 0$, because no deviation of the charge density is present. The potentials satisfy the Lorenz gauge.

Using Eqs. (3) and (4), we obtain the fluctuating electric and magnetic fields whose midplane profiles are shown in Fig. 2. Although the radial and azimuthal components of the fluctuating magnetic field and the axial electric field are present, these are zero only on the midplane because of the symmetry. Those appear in a region near the x-point, where magnetic lines curve. We calculate an electron orbit in the obtained fluctuating field.

3. Electron Orbit Calculation

Electron orbits in the prescribed fluctuating fields are calculated, and the position and particle flux of electrons are summed in the counting cell with a use of the PIC method. The weight of super-particle is set by the Maxwell distribution

$$w = f_M(r, z, v_r, v_\theta, v_z)\, \Delta v_r \Delta v_\theta \Delta v_z\, 2\pi\, r \Delta r \Delta z,$$

where $\Delta v_r = \Delta v_\theta = \Delta v_z = \left(3\sqrt{kT_e/m_e}\right)/N$, and N is the number of velocity segment. In the present study, we set $N = 6$. The lengths Δr and Δz are spacing for super-particle loading in the r and z directions, respectively. Resultantly, the number of super-particles is about 1.4 bil-

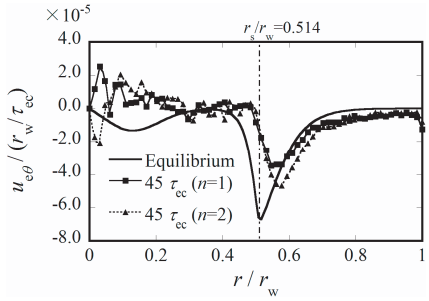

Fig. 3 The midplane profiles of electron toroidal flow velocity. The solid line indicates the equilibrium flow calculated from the Grad-Shafranov equation, the solid line with square makers indicates the $n = 1$ perturbation case, and the dotted line with triangle makers is the $n = 2$ perturbation case.

lion. Coulomb collisions are reproduced by a Monte Carlo method [6].

We suppose that the equilibrium electric field (unperturbed field) is

$$\boldsymbol{E} = -\boldsymbol{u}_\mathrm{e} \times \boldsymbol{B} - \frac{\nabla p_\mathrm{e}}{e n_\mathrm{e}}. \tag{11}$$

The electron toroidal flow velocity is calculated during one cycle of periodic perturbation and shown in Fig. 3. One cycle corresponds to $45\tau_{ec}$, where τ_{ec} is the typical time of electron cyclotron motion and is defined by $\tau_{ec} \equiv m_e r_w^2/(e|\psi_w|)$. By comparing with the equilibrium flow profile, the decrease near the separatrix is significant and the direction of the calculated flow velocity reverses near the geometric axis. The perturbations with the toroidal mode number n of 1 and 2 have almost the same profile, although a faster decay is found for the $n = 1$ perturbation near and outside the separatrix. The flow velocity decay shown in Fig. 3 may correspond to large resistivity. However, when the perturbation is absent, the calculated flow profile is similar to the result seen in Fig. 3. Since the equilibrium electron flow velocity is estimated by neglecting the ion toroidal flow, our result implies that the ion toroidal flow is present in an equilibrium state and the ion current is not negligibly small.

Due to the fluctuating fields, electrons are subject to a periodic force. Since the time-averaged electrical force of oscillating parallel component is zero, it never contributes to heating. The perpendicular velocity component for electrons, however, like magnetic pumping and/or cyclotron heating, gains energy from the perturbation fields. The electron velocity distribution is shown in Fig. 4. The radial and axial velocity distributions are shown in Figs. 4 (a) and (b), respectively. Although the axial velocity distributions at $t = \tau_{ec}$ and $45\tau_{ec}$ are almost the same, however, the distribution broadens with time for the radial velocity distribution that is the perpendicular component. Therefore, it appears that the perturbation energy with the frequency range $\omega \approx 0.1\,\omega_{ec}$ is easily converted to the electron thermal energy.

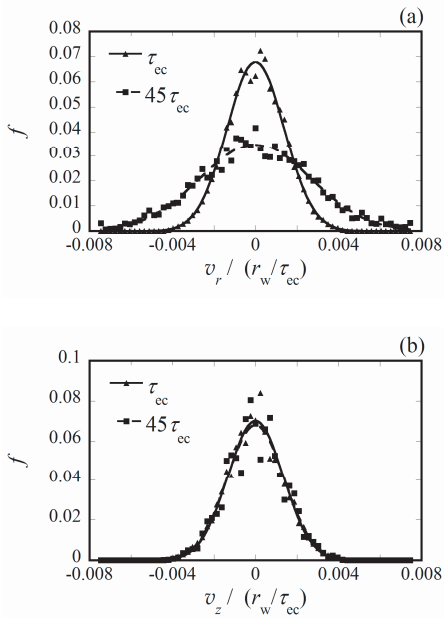

Fig. 4 The electron velocity distributions at the field-null point at 1 (the solid line with triangle markers) and 45 (the dashed line with square markers) electron cyclotron times. (a) The radial velocity distribution, (b) the axial velocity distribution.

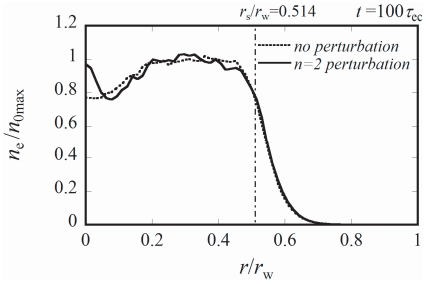

Fig. 5 The midplane profiles of the electron density in the presence of electron fluid perturbation with $n = 2$ (the solid line) and in the absence of perturbation (the dotted line).

The electron density profile on the midplane is presented in Fig. 5, where the density is normalized by the field-null density at $t = 0$. Near the geometric axis $r = 0$, the density increases when the $n = 2$ perturbation fields are added to the equilibrium field. Due to the heating effect by the perturbation field shown in Fig. 4, accessibility of electrons is enhanced and electrons in the neighborhood of and inside separatrix can move toward the separatrix and the geometric axis.

This may also enhances the end-loss rate of electrons. The time evolution of the end-loss electron ratios is shown in Fig. 6. Here, the end-loss ratio is defined as the ratio of the number of end-loss electrons to the whole electrons in the calculation region. The end-loss ratio increases by 53% for the $n = 2$ perturbation case.

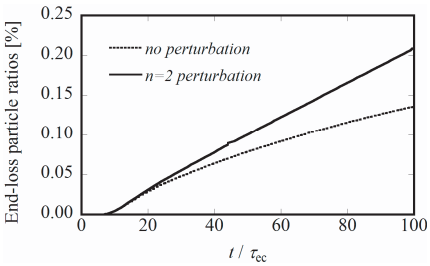

Fig. 6 The time evolution of the end-loss electron ratios for no perturbation (the dotted line) and the $n = 2$ perturbation (the solid line).

4. Summary

The electron fluid perturbation fields have been calculated by assuming that the perturbation originate the electron current fluctuation. Trajectories of electrons in the prescribed perturbation fields have been investigated, and the electron flow and density are calculated by the particle-in-cell method. Although the calculated electron toroidal flow decays rapidly, this may not be attributable to an anomalous resistivity and be attributable to non-negligible ion toroidal flow in an equilibrium state. It is found that due to the perturbation, the perpendicular velocity distribution broadens and electrons are heated. Therefore, it appears that the perturbation energy in the present model is easily converted to the electron thermal energy. Resultantly, electrons near and inside the separatrix can move toward the geometric axis and are lost along an open field line.

Because of the fast conversion of the perturbation energy to the electron thermal energy, a wave with the frequency of $0.1\,\omega_{ec}$ may not survive in FRC plasmas. In order to study the existence of deleterious fluctuating field to transport, we need a self-consistent calculation. We leave this for a future study.

[1] S. Hamasaki and N.A. Krall, *Conference Record of the IEEE International Conference on Plasma Science* (IEEE Publishing Service, Montreal, 1979) p.143.
[2] A.W. Carlson, Phys. Fluids **30**, 1497 (1987).
[3] T. Takahashi *et al.*, Plasma Fusion Res. **2**, 008 (2007).
[4] T. Takahashi *et al.*, Phys. Plasmas **6**, 3131 (2004).
[5] Y. Matsuzawa *et al.*, Phys. Plasmas **15**, 082504 (2008).
[6] A.H. Boozer and G.K.-Petravic, Phys. Fluids **24**, 851 (1981).